# FLOOD EXTENT AND VOLUME CHANGES ANALYSIS IN CURUAI FLOODPLAIN USING REMOTE SENSING

Ana Carolina Pires Pereira, Marie-Paule Bonnet, Frédéric Frappart, Loïc Marie-Louise, Pauline Enguehard, Thibault Catry, Rodrigo Cauduro Dias de Paiva

XXV SIMPÓSIO BRASILEIRO DE RECURSOS HIDRÍCOS

# FLOOD EXTENT AND VOLUME CHANGES ANALYSIS IN CURUAI FLOODPLAIN USING REMOTE SENSING

*Ana Carolina Pires Pereira [1]; Marie-Paule Bonnet [1]; Frédéric Frappart [2]; Loïc Marie-Louise [3]; Pauline Enguehard [1]& Thibault Catry [1]*

**Abstract:** The Amazon is the world's largest watershed and affects the South American and global climate. This region has seen an increase in the recurrence of extreme hydrological events (droughts and floods) in the recent decades. Located near Santarém and Óbidos, where records of maximum level were recently recorded, the Curuai floodplain is about 4,000 km² and is the subject of several studies. Remote sensing is the most appropriate tool for the study of this area due to its complexity and the reduced number of *in situ* measurement stations. The aim of this study was to estimate the flooded extent and volume from Sentinel-1 radar images for two hydrological years (2020-2021 and 2021-2022). For this purpose, an approach based on the classification by the multi-thresholds Otsu method was implemented. The results show that the flood extent varies from 31.58% to 54.85% of the study area and the variation of flooded volume is 19.69 km³. They also show that a larger area is flooded 100% of the time in the hydrological year 2021-2022 than in 2020-2021. The comparison with the literature reinforces facts such as the permanent presence of channels in the south-east and questions the classification by the multi-thresholds Otsu method. The limitations of this methodology open up perspectives for further study with regard to the comparison of several classification methods and the use of altimetry data for the calculation of the depth and, consequently, the flooded volume.

**Keywords** – Amazon, Sentinel-1, multi-thresholds Otsu

## INTRODUCTION

With a surface area of 6 million km², the Amazon watershed is the largest in the world. This unique system has an impact on regional and global climate, providing a source of atmospheric moisture for other regions of the South American continent (Marengo, 2006).

In the Amazon context, floodplains are the part of valleys subject to seasonal flooding that maintain its biodiversity. They act as natural reservoirs and provide ecosystem services. They regulate flooding, affect the flow of carbon, nutrients and sediments, and provide a habitat for numerous plant and animal species (Junk, 1997). The driving force behind all biogeochemical and biological processes in these floodplains is the flood wave, i.e. the fluctuation in water level and the intrusion of water from the associated main river (Junk *et al.*, 1989). The degree of connection between the river and its floodplain is a function of the river's water level: at low water, the floodplain is partially disconnected from the river (Junk, 1997).

Despite the biogeochemical, hydrological and ecosystem importance of floodplains, their extent and the temporal variability of their volume remain not well known (Papa and Frappart, 2021). In tropical zones such as the Amazon, one of the greatest constraints is the difficulty of accessing remote areas, which makes it difficult to carry out *in situ* gauging (flow measurement) and, consequently, to establish the relationships linking height, flow and flooded surface.

1) ESPACE-DEV, IRD, Univ Montpellier, Univ Antilles, Univ Guyane, Univ Réunion, Montpellier, France
2) ISPA, INRAE, Bordeaux Sciences Agro, 33882 Villenave d'Ornon
3) ValorHiz

Due to the complexity of the Amazonian system and the limited number of *in situ* measurement stations, remote sensing has become more widely used. It is very useful for hydrology, and is proving to be the best tool for monitoring the spatio-temporal dynamics of inland waters in the Amazon (Fassoni-Andrade *et al.*, 2021). The Sentinel-1 (S1) mission is a constellation of two satellites that acquire Synthetic Aperture Radar (SAR) images at C-band. The main advantages offered by these data are high spatial resolution (10 m), high revisit frequency (6/12 days in the Amazon basin) and the ability to provide surface information day and night independently of weather conditions, making them useful for a wide range of applications (Filipponi, 2019). The aim of the present study is to analyze a method for classifying S1 images to answer the following questions: (i) what are the different existing DTMs and which one should be chosen for pre-processing S1 images? (ii) what is the variation in flooded area and volume in the Curuai floodplain?; (iii) what is the duration of flooding?; and (iv) in comparison with other studies, are this area and volume underestimated or overestimated?

## STUDY SITE AND DATASETS

### Study site

Located in the low Amazon, close to the cities of Óbidos and Santarém and about 900 km from the mouth of the Amazon, the Curuai floodplain (Figure 1) is composed of several lakes temporarily or permanently interconnected to the main course of the Amazon River by small channels (Bonnet *et al.*, 2008). This complex system of more than 4,000 km² is considered a representative area of the floods in the region and is the subject of many studies (Barbosa, 2007; Bonnet *et al.*, 2008).

The water maximum levels occur between May and July and minimum levels between October and December, when the depths of the main lakes are less than 50 cm (Barbosa, 2007). The two main channels responsible for the floodplain-river connection are about 100 m wide and 3 km long at low water. Their depth varies between 6 m and 12 m. Several other channels gradually connect different parts of the floodplain to the Amazon as the river level rises (Ferreira *et al.*, 2013).

Figure 1 – Location of the Curuai floodplain

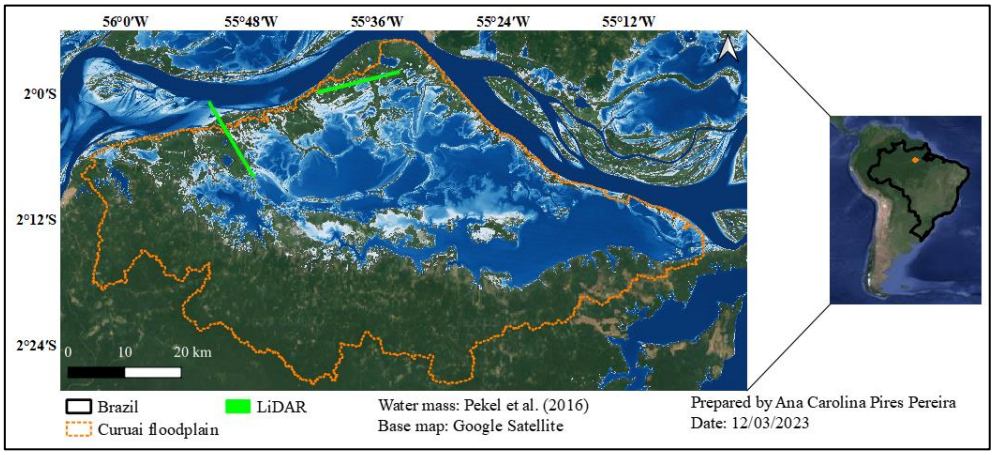


### Digital Elevation Model

In this study, the selection of a Digital elevation model (DEM) aimed to assist in the pre-processing of Sentinel-1 images with respect to terrain correction and calculation of water fill in the Curuai floodplain. Nine DEMs were compared: ALOS, ASTER, Copernicus at 30 m and 90 m spatial resolution, FABDEM, MERIT, MERIT Hydro, SRTM and TanDEM-X.

### Sentinel-1

Sentinel-1 is a constellation composed of two satellites, Sentinel-1A (launched on April 03, 2014) and Sentinel-1B (launched on April 25, 2016), that increases the monitoring of land surfaces including for flood observation. S1 is characterized by a high spatial resolution of 10 m and a revisit time of 6/12 days. Operating at C-band (frequency of 5.405 GHz), S1 is not affected by cloud cover (except in the presence of large water drops) or by weather conditions and can acquire images during both day and night time. Imagery from S1 is freely available and acquisition in VV (vertical transmit and receive) and VH (vertical transmit, horizontal receive) polarizations gives different backscatter responses: greater sensitivity to water roughness in VV, and more volume scattering in VH.

### *In-situ* data

Daily water level data for the Óbidos station were obtained from the Brazilian National Water Agency website (https://www.snirh.gov.br/hidroweb/serieshistoricas). It was used to correct water extent and to estimate the variation in flooded volume.

### Global Surface Water Explorer

Using a Landsat chronology of over thirty years, Pekel *et al.* (2016) mapped the location and distribution of water surfaces. Maximum extent and frequency data were used in this study for comparison with our results.

## MATERIAL AND METHODS

### Difference maps and DEM selection

Difference maps were created using terra package (R Studio, v. 4.2.2) following steps described on Figure 2. A DEM constructed from a combination of GEDI terrain elevation estimates with Copernicus DEM and Landsat surface was taken into account as reference. Difference maps were validated with LiDAR-based high resolution airborne DEMs, acquired by Brazil's National Institute for Space Research between August and September 2016 (Tejada et al., 2019; Urbazaev et al., 2023).

Figure 2 – Steps from creation of difference maps

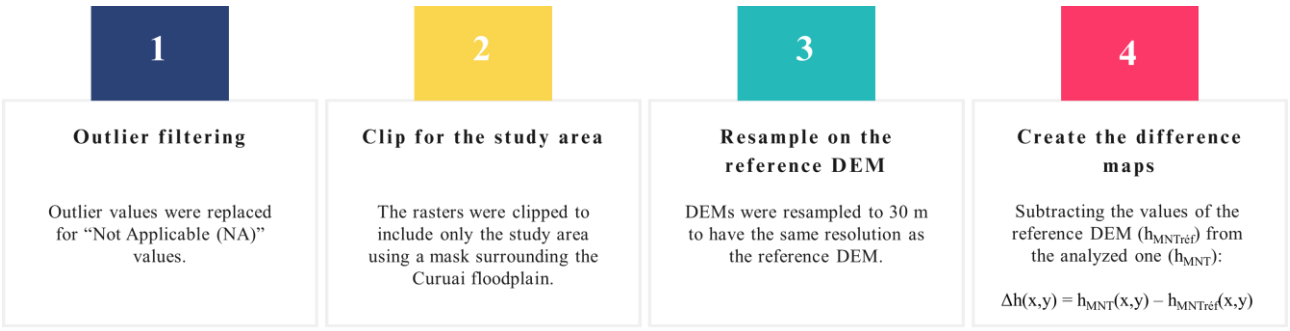


### Delimitation of the flooded area

To facilitate the exploitation of S1 images, a pre-processing was performed using Jupyter notebook (https://jupyter.org/) as a Python interpreter (version 3.6.13). This process consisted of five main steps (Figure 3) using Sentinel Application Platform (SNAP, version 8.0), an open-source Earth observation analysis tool that allows exploration, analysis and processing of remote sensing data (Filipponi, 2019):

Figure 3 – Sentinel-1 images preprocessing workflow


The pre-processed images were then classified using Otsu's thresholding method, a widely used nonparametric thresholding technique (choice of threshold to optimize an objective function) that seeks to define thresholds by maximizing the variance between classes (Otsu, 1979). In this study, two thresholds were determined for each S1 image in order to classify water extent in the Curuai floodplain.

As the study area comprises two different footprints from to S1 orbits, there is a risk of comparing two flooded surfaces that are not comparable if a region contains water in one image and no data in another. A clipping that only takes into account the region common to both areas was carried out and the flooded area in (km²) was calculated (Equation 1).

$$S\ (km^2) = \frac{nº\ pixels\ en\ eau * res.pixel^2}{10^6} \qquad (1)$$

Post-processing was performed to ensure that as the water level at Óbidos increased, the flooded area also increased (and vice versa). Corrections were made for situations where there was an increase in water level accompanied by a reduction in surface area and vice versa. We made the assumption that the surface obtained at low water was probably more accurate than that obtained at high water, given the limitations of the band-C satellite in detecting water under dense vegetation. The date of the minimum surface calculated was determined and corrections were made for two cases: (i) for dates after this date and (ii) for dates before this date.

**Variation in flooded volume**

Firstly, the pixel depth was taken as the difference between the water level at Óbidos and the DTM topography (Equation 2). Then, the variation in the volume of each pixel was calculated as the multiplication between its surface and its depth (Equation 3). Finally, the total variation in flooded volume can be given as the sum of the variation in volume of all pixels in water (Equation 4).

$$H = h_{Óbidos} - h_{FABDEM} \qquad (2)$$
$$\Delta V_{pixel} = S_{pixel} * H = res.pixel^2 * H \qquad (3)$$
$$\Delta V_{tot} = \sum \Delta V_{pixel} \qquad (4)$$

**Flood duration**

Flood duration aims to estimate the number of days per cycle (2020-2021 and 2021-2022) that each pixel is flooded. This calculation considered three steps: (i) reading all the images; (ii) creating a null matrix (all the coefficients have the value zero) to which a unit was added each time a given pixel is flooded in an image (Figure 4); (iii) converting the number of times a pixel is flooded into a number of days by multiplying by the difference in days between the dates of two consecutive images.

Figure 4 – Flood duration matrix update - Diagram for the three-image analysis case.

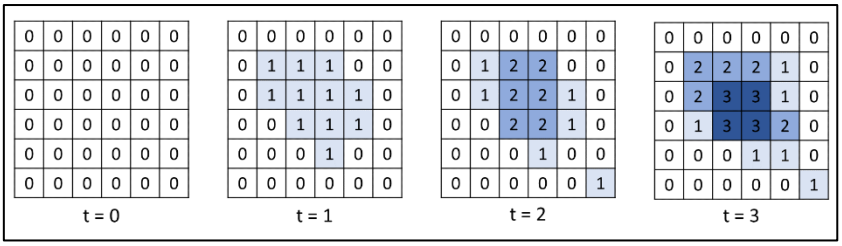


## PRELIMINARY RESULTS

### Difference maps and DEM selection

Difference maps were generated for all nine DEMs considering a range between -5 m and 5 m, illustrated in a scale from blue to yellow (Figure 5). Values lower than -5 m, greater than 5 m and "NA" values are represented in white. Results show that for FABDEM most of the pixels in the study area has difference from referential DEM between the range plotted, especially in the flood zone. In the other hand, results for TanDEM-X show a lot of white regions. The "NA" values, responsible for these white regions, could be explained probably by loss of coherence between the two SAR images due to the presence of vegetation.

Figure 5 – Difference maps for: (a) FABDEM; and (b) TanDEM-X

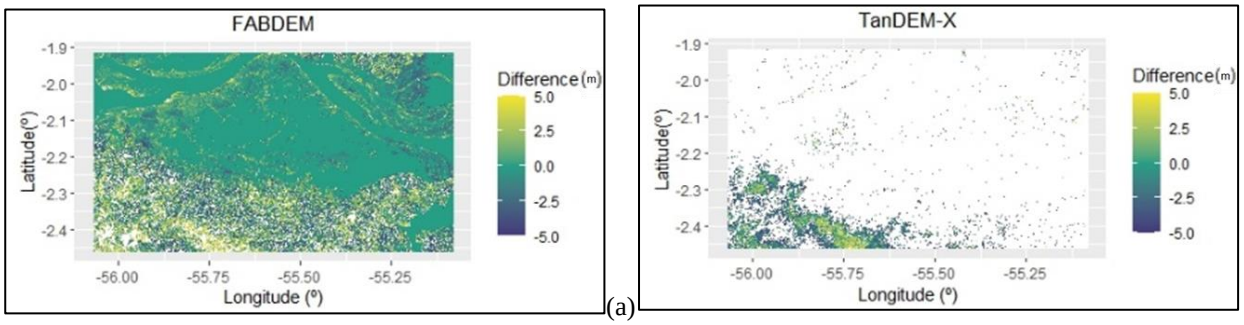


(a) (b)

Descriptive statistics was also considered. Results from minimum, maximum, median, 1st and 3rd quartiles and standard deviation (Table 1) are classified by a color scale: the green indicates the best results, the blue indicates good results and the red represents the worst results. Despite a strong dispersion, the best results are indicated for FABDEM. For this DEM, the results obtained for first quartile, median, third quartile and standard deviation were, respectively, -0.45 m, 0 m, 0.62 m and 2.78 m. Good results for FABDEM were confirmed in comparing this DEM and LiDAR data, so its choice was validated.

Table 1 – Descriptive statistics for all nine DEMs evaluated

| | ALOS | ASTER | Copernicus | | FABDEM | MERIT | MERIT Hydro | SRTM | TanDEM X |
|---|---|---|---|---|---|---|---|---|---|
| | | | 30 m | 90 m | | | | | |
| Min | -70,11 | -78,09 | -21,57 | -26,87 | -32,74 | -32,31 | -34,17 | -39,88 | -105,50 |
| Max | 83,62 | 105,82 | 45,01 | 52,51 | 35,11 | 33,59 | 33,59 | 71,46 | 497,40 |
| Median | -1,13 | 0,18 | 0,18 | 0,39 | 0,00 | 0,13 | -0,40 | -2,50 | -16,60 |
| 1st quartil | -3,22 | -4,50 | 0,00 | 0,00 | -0,45 | -1,43 | -1,70 | -4,50 | -19,90 |
| 3rd quartil | 4,34 | 6,63 | 7,23 | 6,90 | 0,62 | 2,02 | 1,38 | 2,45 | -9,60 |
| Std dev | 6,63 | 7,73 | 5,95 | 5,88 | 2,78 | 3,74 | 3,70 | 5,96 | 9,92 |

## Flood extent

The results presented in this study include the analysis of 59 S1A images in VH polarization. These images correspond to the period between 12/10/2020 and 14/10/2022, i.e. a period of two hydrological cycles. After correction, the extent of 27 images (14 for the first year and 13 for the second) was corrected, with values ranging from 1,784.45 km², for 29/11/2020, to 3,081.39 km², for 11/05/2022 (Figure 5). As the total area evaluated is about 5,650 km², the minimum extent corresponds to 31.58% and the maximum to 54.85% of the image area.

Figure 6 – Water minimum (dark blue) and maximum extend (light blue)

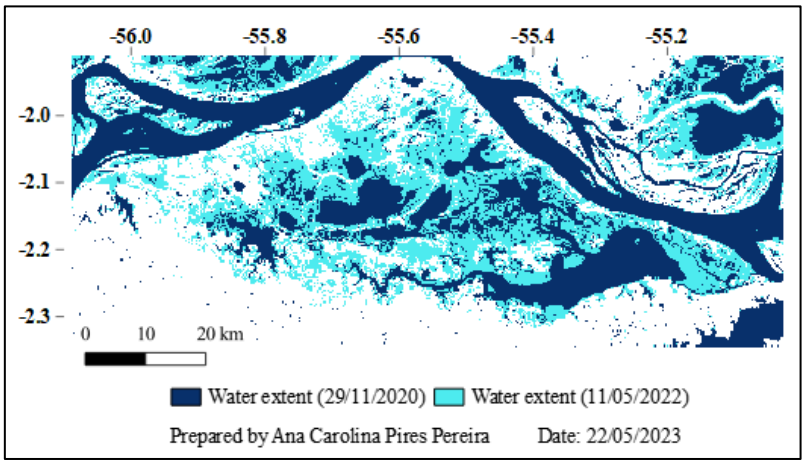


Comparison of the two inundated surfaces (uncorrected and corrected) shows that the post-processing was successful in correcting the surface for the periods before and after 29/11/2020, particularly for the period of rising water. The method used for the correction still a preliminary one, its limitations become obvious from the hypsometric curve (Figure 7). The hysteresis between flows and inundated surfaces between the period of rising and receding water has already been reported for the Óbidos region (Rudorff *et al.*, 2014). However, the variations here between these periods appear to be overestimated. For high water (level around 800 cm) and for low water (level less than 200 cm), close surface values were found. For values between 200 and 800 cm, oscillations were observed: a difference of almost 300 km² was observed for a level of 486 cm. Future improvements will be made to make the post-processing more robust, for example by comparing each image with the previous and subsequent images and ensuring that for similar levels, the areas are also similar.

Figure 7 – Hypsometric curve relating water levels and flooded surfaces

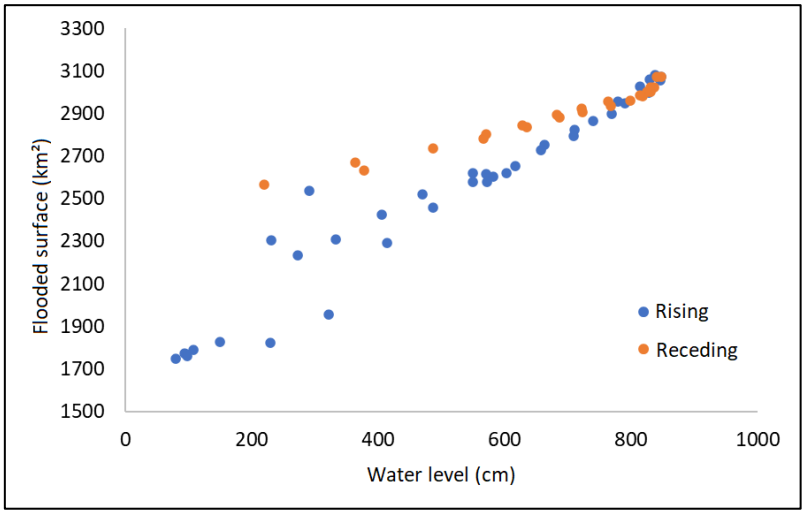

## Variation in flooded volume

The volume estimated after the surface correction varies from 1.89 km³, for 05/11/2020, to 21.58 km³, for 28/05/2021 (Figure 8), the dates of the minimum and maximum water levels, this corresponds to a maximum variation of 19.69 km³. As the high-water period has a greater flooded area (number of pixels in water) and higher water levels, it was expected that the volume curve would follow the same pattern as these curves. The lowest volumes are observed at the end of 2020, with the two peaks representing high water in 2021 and 2022, respectively. A plateau is observed at the beginning of 2022, with volumes of between 14.48 km³ and 14.78 km³.

The dates corresponding to the minimum and maximum volumes coincide with the dates of the minimum and maximum water levels, which was expected, since we do not consider vertical variation in flooding. This is a source of uncertainty in the estimation; more accurate results can be obtained by taking into account heights that vary by pixel. Other sources of uncertainty in this estimate are related to the uncertainties in S1 images and the construction of the FABDEM.

Figure 8 – Time variations in flooded volume between 12/10/2020 and 14/10/2022

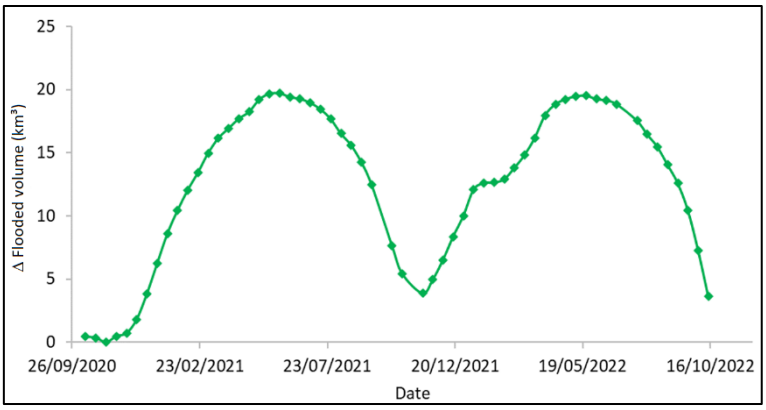


## Flood duration

The duration of flooding per pixel was plotted for each hydrological year studied (Figure 9). It shows a greater number of pixels permanently flooded (100% of the year) for the period 2021-2022 than for the period 2020-2021. The probable explanation is related to the lower water level in the second hydrological year: the minimum water level was higher in 2021-2022 (220 cm) than in 2020-2021 (79 cm), so more pixels were not covered with water in 2020-2021.

Figure 9 – Flood duration for 2020-2021 (left) and for 2021-2022 (right)

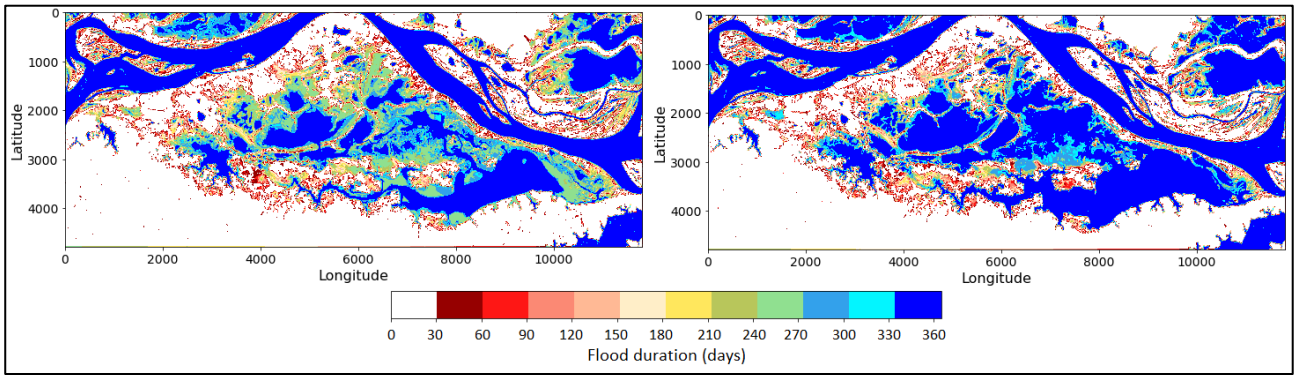


The two duration maps reinforce the expected patterns: the Amazon and Tapajós rivers are permanently covered with water, as are the channels in the south-eastern part; the central part fills up

with water from the middle to the shores; the north-western part has a lower flooding duration throughout the year; and the southern part, corresponding to the terra firma regions, never flooded.

**Discussion**

The flooding patterns observed in this study are consistent with previous studies, which indicate that the two main channels responsible for permanently linking the Curuai floodplain to the Amazon are located in the south-eastern part of the floodplain (Bonnet *et al.*, 2008; Ferreira *et al.*, 2013). The dates of the maximum and minimum areas are consistent with the literature. Previous studies indicate that maximum water levels and surfaces in the region occur between May and July, with a lag of around three months compared with the peak of the rainy season, which takes place between February and April, and the lowest water levels and surfaces are generally observed between October and November (Arnesen *et al.*, 2013; Rudorff *et al.*, 2014).

The differences observed can be attributed to factors such as area and study period and datasets. A greater extent and volume are expected for studies like ours, which consider Amazon and Tapajós rivers, than for studies that consider only the Curuai area, as is the case of Bonnet *et al.* (2008) and Rudorff *et al.* (2014). The lower amplitude of variation between low and high water in our study is explained by the inclusion of these rivers, which are permanent waters, but also because the period covered, Bonnet *et al.* (2008) for example includes both dry (1997) and very wet (1999) years. In comparison with Arnesen *et al.* (2013), a smaller area to the north and north-west of the plain was delineated. These differences are partly explained by the fact that ALOS-PALSAR (L-band radar) can detect water under even dense vegetation, which is not necessarily the case for Sentinel-1 (C-band radar).

The maximum extent was compared with that of Pekel *et al.* (2016). Presented in a scale varying from black to blue, the difference map (Figure 10) highlights pixels with no data recorded by S1 in black (value equal to -2), "underestimates" in red (value equal to -1), identical values in white (value equal to 0) and "overestimates" in blue (value equal between 1). In total, 92.60% of pixels have the same value, either water in both cases, or no water in both cases.

Flood duration values were reported as percentages for comparison with flood frequency data proposed by Pekel *et al.*, (2016). In 2021-2022 (Figure 10), the number of overestimated pixels was 8.9%, while the number of underestimated pixels was 8.6%: 17.5% of pixels therefore had different values to those of Pekel *et al.* (2016). 82.5% of pixels had the same flood frequency as Pekel *et al.* (2016) for this hydrological year.

Figure 10 – Comparison with Pekel et al. (2016) - Difference map between the maximum extent estimated (left) and flood frequencies estimated for the 2021-2022 hydrological year (right).

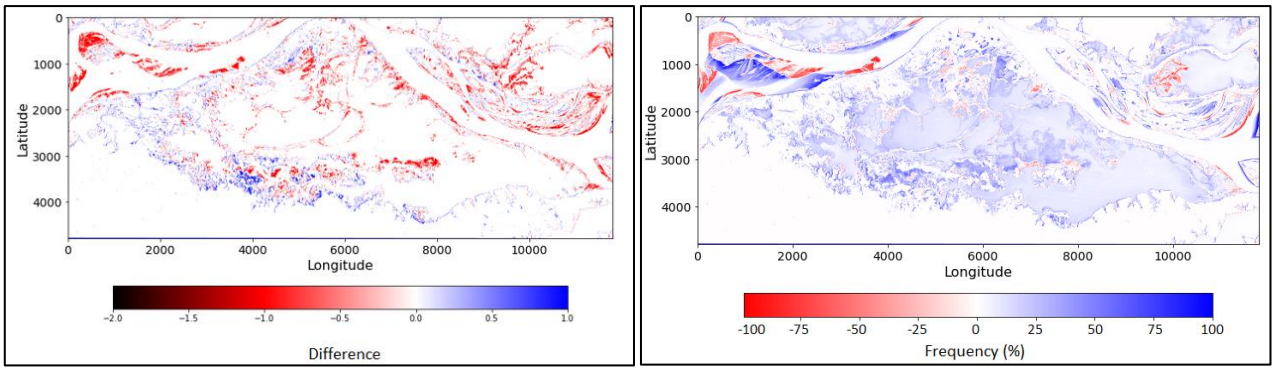


Some of the observed differences can be explained by the water detection capability under vegetation of the SAR C-band and optical sensors used by Pekel *et al.* (2016), as the optical sensor

cannot detect water under vegetation, while the C-band radar can detect water under sparse vegetation. We would therefore have expected to obtain more overestimated pixels than underestimated ones. On the other hand, the product of Pekel *et al.* (2016) may include flood peaks larger than those we studied. It is likely, however, that the classification method used slightly underestimates the water extent.

## CONCLUSIONS AND PERSPECTIVES

In tropical regions with few *in situ* gauges, such as the Amazon, satellite remote sensing is the only approach that can provide continuous comprehension of spatio-temporal dynamics of floodplains (Jensen *et al.*, 2018). This region is considered as an ideal natural laboratory for remote sensing studies: characterized by high rates of precipitation and evapotranspiration, as well as changes in water storage and flow, the development of remote sensing techniques in the world's largest river basin improves our understanding of the hydrological processes taking place there (Fassoni-Andrade *et al.*, 2021).

Floodplains play a major role in the functioning of the Amazonian hydrosystem. Enriched with sediment, they are ideal for agriculture and farming during low-water periods. A highly dynamic environment, vegetation is born at each low-water period and dies at each flood season. Identifying and characterizing flood-prone areas is therefore both technically and socially interdisciplinary.

This study implemented a methodology of pre-processing, classification and post-processing of S1 imagery in order to characterize flooding in the Curuai floodplain in terms of extent, volume and duration. The results show consistency with the literature regarding flooded areas at low and high water, as well as lower and higher surface and volume date (Bonnet *et al.*, 2008; Arnesen *et al.*, 2013; Rudorff *et al.*, 2014). A comparison with maps of frequency and maximum flood extent (Pekel et al., 2016) was made and highlighted important differences. Concerning frequency, for example, overestimates of up to 100% were observed.

Improvements to the methodology can be envisaged. The classification method can be compared with other unsupervised classification methodologies and the use of the two polarizations VV and VH and their ratio. To refine the volume calculation, non-constant water heights over the study area, derived from altimetry satellites, can be used. With the results of a solid and robust methodology, I hope that the research begun with this study can have a social purpose in line with the work developed with local communities.

## REFERENCES

ARNESEN, A.S.; SILVA, T.S.F.; HESS, L.L.; NOVO, E.M.L.M.; RUDORFF, C.M.; CHAPMAN, B.D.; MCDONALD, K.C. (2013). *"Monitoring flood extent in the lower Amazon River floodplain using ALOS/PALSAR ScanSAR images"*. Remote Sensing of Environment, 130, pp. 51-61.

BARBOSA, C.C.F. (2007). *"Sensoriamento remoto na dinâmica da circulação da água do sistema Planície de Curuai/Rio Amazonas"*.

BONNET, M.P.; BARROUX, G.; MARTINEZ, J.M.; SEYLER, F.; MOREIRA-TURCQ, P.; COCHONNEAU, G.; MELACK, J.M.; BOAVENTURA, G.; MAURICE-BOURGOIN, L.; LEÓN, J.G.; ROUX, E.; CALMANT, S.; KOSUTH, P.; GUYOT, J.L.; SEYLER, P. 2008. *"Floodplain hydrology in an Amazon floodplain lake (Lago Grande de Curuaí)"*. Journal of Hydrology, 349(1-2), pp. 18-30.

FASSONI-ANDRADE, A.C.; FLEISCHMANN, A.S.; PAPA, F.; PAIVA, R.C.D.; WONGCHUIG, S.; MELACK, J.M.; MOREIRA, A.A.; PARIS, A.; RUHOFF, A.; BARBOSA, C.; MACIEL, D.A.; NOVO, E.; DURAND, F.; FRAPPART, F.; AIRES, F.; ABRAHÃO, G.M.; FERREIRA-

FERREIRA, J.; ESPINOZA, J.C.; LAIPELT, L.; COSTA, M.H.; ESPINOZA-VILLAR, R.; CALMANT, S.; PELLET, V. (2021). *"Amazon Hydrology From Space: Scientific Advances and Future Challenges"*. Reviews of Geophysics, 59(4).

FERREIRA, R.D.; BARBOSA C.C.F.; NOVO, E.M.L.M. (2013). *"Assessment of in vivo fluorescence method for chlorophyll-a estimation in optically complex waters (Curuai floodplain, Pará - Brazil)"*. Acta Limnologica Brasiliensia, 24(4), pp. 373-386.

FILIPPONI, F. (2019). *"Sentinel-1 GRD Preprocessing Workflow"*. International Electronic Conference on Remote Sensing. 3rd International Electronic Conference on Remote Sensing, pp. 11.

JENSEN, K.; MCDONALD, K.; PODEST, E.; RODRIGUEZ-ALVAREZ, N.; HORNA, V.; STEINER; N. (2018). *"Assessing L-Band GNSS-Reflectometry and Imaging Radar for Detecting Sub-Canopy Inundation Dynamics in a Tropical Wetlands Complex"*. Remote Sensing, 10(9), pp. 1431.

JUNK, W.J. (1997). *"The Central Amazon Floodplain"*. Berlin, Heidelberg: Springer Berlin Heidelberg (Ecological Studies).

JUNK, W.; BAYLEY, P.B.; SPARKS, R.E. (1989). *"The flood pulse concept in river-floodplain systems"*. D.P. Dodge, ed. Proceedings of the International Large River Symposium (LARS). Canadian Special Publication of Fisheries and Aquatic Sciences, 106, pp. 110-127.

MARENGO, J.A. (2006). *"On the hydrological cycle of the Amazon Basin: a historical review and current state-of-the-art"*. Revista Brasileira de Meteorologia, 21.

OTSU, N. (1979). *"A Threshold Selection Method from Gray-Level Histograms"*. IEEE Transactions on Systems, Man, and Cybernetics, 9(1), pp. 62-66.

PAPA. F.; FRAPPART, F. (2021). *"Surface Water Storage in Rivers and Wetlands Derived from Satellite Observations: A Review of Current Advances and Future Opportunities for Hydrological Sciences"*. Remote Sensing, 13(20), pp. 4162.

PEKEL, J.F.; COTTAM, A.; GORELICK, N.; BELWARD, A.S. (2016). *"High-resolution mapping of global surface water and its long-term changes"*. Nature, 540(7633), pp. 418-422.

RUDORFF, C.M.; MELACK, J.M.; BATES, P.D. (2014). *"Flooding dynamics on the lower Amazon floodplain: 2. Seasonal and interannual hydrological variability: lower Amazon floodplain hydrological variability"*. Water Resources Research, 50(1), pp. 635-649.

TEJADA, G.; GÖRGENS, E.B.; ESPÍRITO-SANTO, F.D.B.; CANTINHO, R.Z.; OMETTO, J.P. (2019). *"Evaluating spatial coverage of data on the aboveground biomass in undisturbed forests in the Brazilian Amazon"*. Carbon Balance and Management 14(1), pp. 11.

URBAZAEV, M.; HESS, L.L.; OMETTO, J.P.; SCHMULLIUS, C. (2023). *"Combining GED, the Copernicus GLO-30 DEM, and Landsat data to generate a bare-earth digital model terrain for the mid-Juruá region"*.

## ACKNOWLEDGMENTS

This work was supported by some projects: BONDS (financed by the French National Research Agency, FAPESP, National Science Foundation, the Research Council of Norway and the German Federal Ministry of Education and Research), SABERES (financed by the BNP Paribas Foundation as part of its "Climate & Biodiversity Initiative" program 2019), INCT-Odisseia, French *Centre National d'Etudes Spatiales* (CNES) projects TOSCA and SWHYM, and PROGYSAT from *Programme de Coopération Interreg Amazonie* (PCIA).